



Article

The Major Heat Shock Proteins, Hsp70 and Hsp90, in 2-Methoxyestradiol-Mediated Osteosarcoma Cell Death Model

Magdalena Gorska-Ponikowska ^{1,*}, Alicja Kuban-Jankowska ¹ ,
Antonella Marino Gammazza ^{2,3}, Agnieszka Daca ⁴ , Justyna M. Wierzbicka ⁵ ,
Michal A. Zmijewski ⁵ , Hue H. Luu ⁶, Michal Wozniak ¹ and Francesco Cappello ^{2,3}

¹ Department of Medical Chemistry, Medical University of Gdansk, 80-211 Gdansk, Poland; alicjakuban@gumed.edu.pl (A.K.-J.); mwozniak@gumed.edu.pl (M.W.)

² Euro-Mediterranean Institute of Science and Technology, 90127 Palermo, Italy; antonella.marino@hotmail.it (A.M.G.); francescocappello@iemest.eu (F.C.)

³ Department of Biomedicine, Neurosciences and Advanced Diagnostics (BiND), University of Palermo, 90127 Palermo, Italy

⁴ Department of Pathology and Experimental Rheumatology, Medical University of Gdansk, 80-211 Gdansk, Poland; agnieszka.ela@gumed.edu.pl

⁵ Department of Histology, Medical University of Gdansk, 80-211 Gdansk, Poland; jwierzbicka@gumed.edu.pl (J.M.W.); mzmijewski@gumed.edu.pl (M.A.Z.)

⁶ Department of Orthopaedic Surgery and Rehabilitation Medicine, University of Chicago, Chicago, IL 60637, USA; hluu@surgery.bsdu.uchicago.edu

* Correspondence: magdalena.gorska-ponikowska@gumed.edu.pl

Received: 19 November 2019; Accepted: 14 January 2020; Published: 17 January 2020



Abstract: 2-Methoxyestradiol is one of the natural 17β -estradiol derivatives and a potential novel anticancer agent currently being under evaluation in advanced phases of clinical trials. However, the mechanism of anticancer action of 2-methoxyestradiol has not been yet fully established. In our previous studies we have demonstrated that 2-methoxyestradiol selectively induces the expression and nuclear translocation of neuronal nitric oxide synthase in osteosarcoma 143B cells. Heat shock proteins (Hsps) are factors involved in the regulation of expression and activity of nitric oxide synthases. Herein, we chose osteosarcoma cell lines differed in metastatic potential, metastatic 143B and highly metastatic MG63.2 cells, in order to further investigate the anticancer mechanism of 2-methoxyestradiol. The current study aimed to determine the role of major heat shock proteins, Hsp90 and Hsp70 in 2-methoxyestradiol-induced osteosarcoma cell death. We focused on the implication of Hsp90 and Hsp70 in control under expression of neuronal nitric oxide synthase, localization of the enzyme, and further generation of nitro-oxidative stress. To give the insight into the role of Hsp90 in regulation of anticancer efficacy of 2-methoxyestradiol, we used geldanamycin as a potent Hsp90 inhibitor. Herein, we evidenced that inhibition of Hsp90 controls the protein expression of 2-methoxyestradiol-induced neuronal nitric oxide synthase and inhibits enzyme nuclear translocation. We propose that decreased level of neuronal nitric oxide synthase protein after a combined treatment with 2-methoxyestradiol and geldanamycin is directly associated with the accompanying upregulation of Hsp70 and downregulation of Hsp90. This interaction resulted in abrogation of anticancer efficacy of 2-methoxyestradiol by geldanamycin.

Keywords: 2-methoxyestradiol; geldanamycin; neuronal nitric oxide synthase; osteosarcoma

1. Introduction

Osteosarcoma (OS) is one of the most malignant childhood bone tumors [1–3]. Clinically ineffective treatment of osteosarcoma is often associated with the high metastatic potential of the tumor and substantial chemoresistance [1–3]. Thus, searching for novel, potent anticancer drugs is a challenging scientific task of highest priority.

In our previous studies using OS cell lines we established that an anticancer agent potentially effective in therapy of osteosarcoma is 2-methoxyestradiol (2-ME) [4–9].

2-ME is one of the natural 17β -estradiol derivatives. 2-ME is also candidate for a being novel anticancer agent [10–19]. Preclinical research suggests a wide spectrum of possible anticancer mechanisms of 2-ME action that seem to be directly associated with the inhibition of angiogenesis and induction of apoptosis in tumorous and proliferating cells [20–25]. Notably, normal cells are more resistant to proapoptotic properties of 2-ME [26,27].

Consequently, 2-ME has been evaluated in different phases of clinical trials considering treatment of various cancers [9–19], including sarcoma [16]. However, 2-ME is characterized by unfavorable pharmacokinetic profile [10,16,19], therefore currently new formulations of 2ME are currently being developed with the intent of increasing oral bioavailability.

Based on our previous studies we evidenced that from a mechanistic point of view, 2-ME specifically induces the expression and nuclear translocation of neuronal nitric oxide synthase (nNOS) [4–9]. There can be distinguished three isoforms of nitric oxide synthases (NOSs), namely nNOS (neuronal nitric oxide synthase, Type I, NOS-1, NOS-I) found mainly in neurons, iNOS (inducible nitric oxide synthase, Type II, NOS-2, NOS-II) induced by many stimuli like stress or inflammation in different kinds of cells and tissues, and eNOS (endothelial nitric oxide synthase, Type III, NOS-3, NOS-III) expressed mainly in endothelial cells [28,29]. nNOS is constitutively expressed mainly in brain tissues, but similarly was found in a spinal cord, adrenal and ganglia glands, peripheral nitrergic nerves, kidneys, pancreatic cells, and interestingly in vascular smooth, skeletal muscles and cardiac myocytes [28–30]. Regulation of NOSs occurs at the levels of enzyme activity and mRNA synthesis. The nNOS mRNA is structurally diverse as a consequence of alternative promoters and alternate splicing [31]. Notably, nNOS is a larger protein than either eNOS and iNOS because of the N-terminal extension that contains a PDZ domain, a consensus sequence of approximately 90 amino acids, that has been shown to mediate protein-protein interactions (e.g., with PSD93/95, CAPON, phosphofructokinase) [28,32].

Nuclear localization of nNOS in 2-ME-treated osteosarcoma cells leads to local nitric oxide synthesis and DNA damage, and finally, resulting in cancer and actively dividing cell death [7,8,33]. Currently, the mechanism underlying on the induction of nNOS by 2-ME has not been established.

Heat shock proteins (Hsps) are factors involved in the regulation of expression and activity of NOSs [34–40]. Hsps regulate the activity of NOSs and therefore may limit the production of nitric oxide and its derivatives. The Hsp70/Hsp90 chaperone machinery is responsible for the triage decision concerning protein quality and their proteasomal ubiquitination. Notably, the oxygenase domain of nNOS with the heme/substrate binding cleft is the site of interaction with Hsp90 protein [35]. Garcia-Cardena et al. revealed the activation of purified eNOS by Hsp90 in the absence of heme and cofactors. They further proved that Hsp90 is an allosteric activator of eNOS [35]. Notably, Hsp90 may also activate nNOS isoform [36]. Similarly to Hsp90, Hsp70 possesses the same binding site within the oxygenase domain of nNOS [37]. Therefore, the overexpression of Hsp70 in contrast to Hsp90, promotes ubiquitination and proteasomal degradation of nNOS [37,38].

There is also a paucity of data demonstrating the role of Hsp70 in the regulation of nNOS activity [36–40]. It was further proposed that Sp and ZNF families transcription factors, together with Oct-2, are potential candidates via which HSP70 may regulate nNOS gene expression [40].

Therefore, the aim of the study was to investigate the role of major Hsps in 2-ME anticancer mode of action focusing on the mechanisms relying on the regulation of nNOS expression and its nuclear translocation. We further investigated whether abrogation of Hsp90 by geldanamycin, potent Hsp90

inhibitor [41], may interfere with anticancer efficacy of 2-ME which may be at least partially associated with expression and localization of nNOS enzyme.

In the current study we used human metastatic OS 143B cells with established molecular response to treatment with 2-ME [4–9]. In addition, the data were supported by results obtained on highly metastatic mice OS MG63.2 cells [42,43]. A highly metastatic subline MG63.2 was established by member of our team from the occasional pulmonary metastases developed from MG63 in mice [42–44].

2. Results

2.1. Anti-Proliferative Effect of 2-ME and GA

First goal of the study was to investigate whether GA impacts on anti-proliferative activity of 2-ME using metastatic 143B and highly metastatic MG63.2 cell lines.

143B and MG63.2 cells were treated with series of dilutions (0.8 μM –50 μM) of either 2-ME or GA, or a combination of both for 24 h. Subsequently, the inhibition of 143B and MG63.2 cell growth was observed by means of MTT-assay.

As demonstrated in Figure 1, both 2-ME and GA effectively inhibited cell growth of OS in a concentration- and cell-dependent manner.

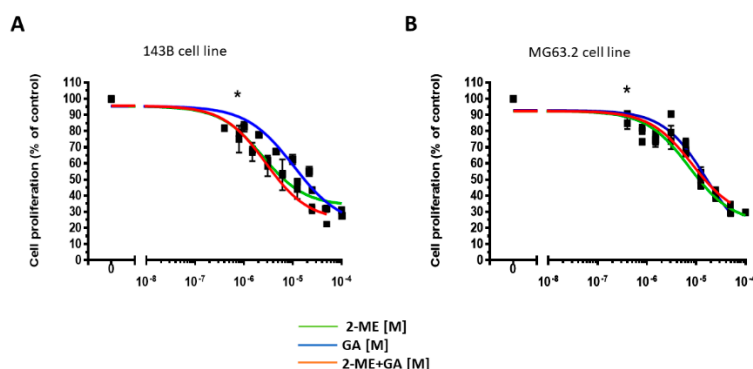


Figure 1. Anti-proliferative effects of 2-methoxyestradiol (2-ME) and GA in 143B and MG63.2 cell lines. Anti-proliferative effect of 2-ME or GA, or a combination of both compounds in OS 143B and MG63.2 cells. OS 143B (A) and M63.2 (B) were treated with series of dilutions (0.8 μM –50 μM) of either 2-ME or GA, or a combination of both (molar ratio 1:1). The cell proliferation was consequently determined by MTT assay. Data are presented as the mean \pm SE values from at least three independent experiments. The absence of error bar denotes a line thickness greater than the error. Data were analyzed by GraphPad Prism Software version 6.02 performing One-way ANOVA combined with Dunnett’s Multiple Comparison Test. * $p < 0.01$ versus control.

Viability of 143B cells was significantly diminished from 81% to 31% (Figure 1A), whereas MG63.2 cells from 82% to 29% (Figure 1B) in the presence of series of dilutions of 2-ME (0.8 μM –50 μM) as compared to control, respectively. Survival of 143B was reduced from 77.28% to 23.1% (Figure 1A) while MG63.2 from 90.6% to 29.8% (Figure 1B) in the presence of series of dilutions of GA (0.8 μM –50 μM) as compared to control.

Subsequently, 143B and MG63.2 cells were treated with combination of 2-ME and GA (concentrations range 0.8 μM –50 μM , molar ratio 1:1). The combined treatment with 2-ME and GA on both 143B and MG63.2 cells resulted in comparable anti-proliferative effects to compounds when used separately (Figure 1A,B, indicated as red color). Specifically, treatment of 143B cell line with 2-ME and GA in combination resulted in inhibition of cell proliferation from 58.3% to 21.4% (Figure 1A). While viability of MG63.2 was diminished from 68% to 29.2% (Figure 1B).

Notably, as indicated by calculated EC₅₀ values, MG63.2 cell line is approximately 10 times more resistant in comparison to 143B cell line. These results confirm high metastatic potential of MG63.2 cell line. Specifically, the EC₅₀ values calculated for 2-ME and GA in OS 143B were equal to 0.42 μM and

1.3 μM , respectively; while in MG63.2 were equal to 4.21 μM and 15.8 μM , respectively. While, EC50 values calculated for combination of 2-ME and GA in 143B and MG63.2 cells were at the similar level as compared to separate treatment—1.12 μM and 15.1 μM , respectively.

2.2. A Quantitative Measure of the Degree of Drug Interaction

We have further quantitatively evaluated the degree of 2-ME and GA interaction in OS 143B cells as representative cell line using CalcuSyn software [45]. Based on the results of MTT assay, we evaluated the median-effect plot, dose–effect curve and Fa-CI plot (Figure 2).

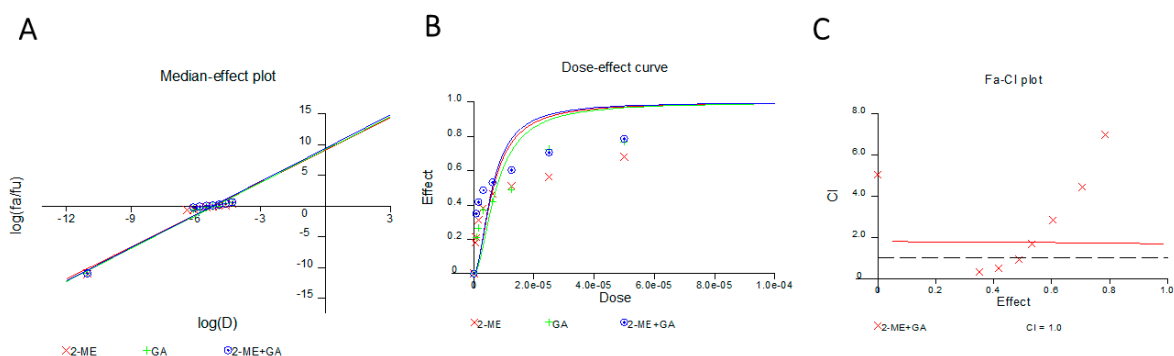


Figure 2. Antagonistic effect between 2-ME and GA. Anti-proliferative potential of 2-ME (red line), GA (green line), and the combination of both compounds (blue line) was determined by MTT assay as described above. Consequently, median-effect plot (A), dose–effect curve (B), and Fa-CI plot (C) were evaluated by CalcuSyn software. Values are the mean \pm SE from three independent experiments.

The calculated combination index (CI) for mixture of 2-MA and GA (molar ratio 1:1) at ED50, ED75 and ED90 was equal to 1.76165, 1.74029, 1.71927 ($r = 0.98$), respectively. CI more than 1 which clearly indicates antagonism between compounds. The calculated D_m value for combination of 2-ME and GA was equal to 6.05×10^{-6} ($6.05e^{-6}$) while m was value more than 1.7 indicates the hyperbolic dose–effect curve (Figure 2).

2.3. Antagonistic Effect of 2-ME and GA in Osteosarcoma Cell Death Model

In order to further investigate the interaction between 2-ME and GA, we consequently investigated the impact of the compounds on induction of OS 143B and MG 63.2 cell death using flow cytometry. Based on the obtained anti-proliferative data and our previous studies [4–8], we chose the representative concentrations of 2-ME equaled to 1 μM or 10 μM ; while of GA equaled to 2 μM or 4 μM for the following studies.

To determine the influence of 24 h long treatment with either 2-ME (1 μM or 10 μM) or GA (2 μM or 4 μM), or a combination of both on induction of cell death in OS cells, flow cytometric-double staining (Annexin V and PI) was performed.

As presented in Table 1, an increase in apoptotic and necrotic 143B and MG63.2 cell number resulted from 2-ME (1 μM or 10 μM) or GA (2 μM or 4 μM), treatment was observed. Next goal of the study was to determine the effect of combined treatment with 2-ME and GA on cell death induction regarding to metastatic potential of OS 143B and MG63.2 cell lines. Notably, no significant differences between the combined and separate treatments with 2-ME and/or GA in induction of apoptosis and necrosis were observed (Table 1).

Similarly to previous results, MG63.2 cell line was more resistant to treatment with 2-ME or GA as compared with 143B cell line. Due to the obtained results, lack of synergistic effects of 2-ME and GA in employed OS cell death model may be confirmed.

Table 1. Antagonistic effects of 2-ME and GA in 143B and MG63.2 cell lines.

Compound	143B Cell Line		MG63.2 Cell Line	
	% of Apoptotic Cells	% of Necrotic Cells	% of Apoptotic Cells	% of Necrotic Cells
Control	3% ± 1.5	5% ± 1.3%	5% ± 1.2%	4% ± 2.3%
1 μM 2-ME	13% ± 3.3% * <i>p</i> < 0.01	13.2% ± 5% * <i>p</i> < 0.01	9.4% ± 2.4% * <i>p</i> < 0.01	10.71 ± 1.3% * <i>p</i> < 0.01
10 μM 2-ME	36% ± 11% **** <i>p</i> < 0.00001	28.5% ± 13% **** <i>p</i> < 0.00001	17.2% ± 2.5% ** <i>p</i> < 0.001	16.4% ± 4.2% *** <i>p</i> < 0.0001
2 μM GA	17.5% ± 1% * <i>p</i> < 0.01	23.3% ± 8.3% ** <i>p</i> < 0.001	19.6% ± 2.8% **** <i>p</i> < 0.00001	15.6% ± 3.9% *** <i>p</i> < 0.0001
4 μM GA	41.5% ± 9% **** <i>p</i> < 0.00001	21.5% ± 3.8% * <i>p</i> < 0.01	20% ± 2.5% **** <i>p</i> < 0.00001	16.5% ± 5.2% **** <i>p</i> < 0.00001
1 μM 2-ME + 2 μM GA	25.2% ± 7.4% * <i>p</i> < 0.01	23.9% ± 6.8% ** <i>p</i> < 0.001	23.6% ± 3.7% **** <i>p</i> < 0.00001	15% ± 6.6% ** <i>p</i> < 0.001
1 μM 2-ME + 4 μM GA	40% ± 14.8% **** <i>p</i> < 0.00001	19.3% ± 6.2% * <i>p</i> < 0.01	22.9% ± 4.3% **** <i>p</i> < 0.00001	17.9% ± 1.2% *** <i>p</i> < 0.0001
10 μM 2-ME + 2 μM GA	28% ± 14% *** <i>p</i> < 0.0001	22% ± 5.3% ** <i>p</i> < 0.001	21.5% ± 3.5% **** <i>p</i> < 0.00001	17.5% ± 1.5% *** <i>p</i> < 0.0001
10 μM 2-ME + 4 μM GA	39.3% ± 10.2% **** <i>p</i> < 0.00001	25.5% ± 3.1% ** <i>p</i> < 0.001	26.4% ± 1.4% **** <i>p</i> < 0.00001	13.01% ± 1.7% * <i>p</i> < 0.01

Induction of cell death by 2-ME, GA or combination of both compounds in OS 143B and MG63.2 cells. 143B and MG63.2 OS cells were treated with vehiculum (Control cells), 2-ME (1 μM, 10 μM) or GA (2 μM, 4 μM) or combination of both for 24 h. The cells were then harvested and the percentage of apoptotic and necrotic cells was determined using Annexin V-PI staining by flow cytometry. Values are the mean ± SE of three independent experiments (N = 6 replicate cultures). Data were analyzed by GraphPad Prism Software version 6.02 performing one way ANOVA analyses followed by Tukey's multiple comparison test. * *p* < 0.01, ** *p* < 0.001, *** *p* < 0.0001, **** *p* < 0.00001 versus control.

2.4. GA Decreased 2-ME Mediated Overexpression and Nuclear Translocation of nNOS

We further verified our hypothesis whether nNOS can be directly associated with the antagonistic effect between 2-ME and GA in OS 143B and MG63.2 cells. As we have previously reported, the highest level of nNOS associated with nitric oxide generation observed after treatment with 2-ME was detected between 6 h and 8 h [4–8]. Therefore herein OS 143B and MG63.2 cells were treated with either 2-ME (1 μM or 10 μM) or GA (2 μM or 4 μM), or a combination of both for 8 h. nNOS protein level was then determined by Western blotting and immunofluorescence (Figures 3 and 4).

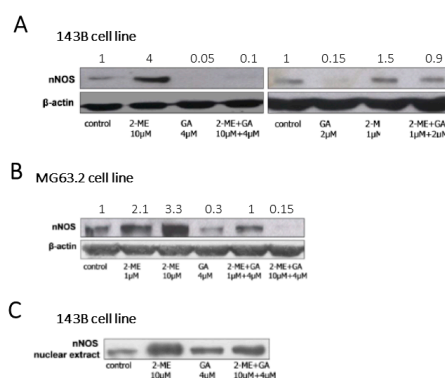


Figure 3. GA abrogates stimulatory effect of 2-ME on nNOS expression and nuclear translocation in 143B and MG63.2 cell lines. Total pool of nNOS in OS 143B (A), MG63.2 (B) cells and in nuclear extract of 143B cells (C) treated with either 2-ME or GA, or a combination of both compounds. 143B and MG63.2 OS cells were treated with vehiculum (Control), 2-ME (1 μM, 10 μM) or GA (2 μM, 4 μM) or combination of both for 8 h. The cells were then harvested and total level of nNOS was established by western blotting. The cytoplasmic and nuclear fractions were separated using the Nuclear Extract Kit (Active Motif, France) according to manufacturer's protocol. The representative data from three experiments are presented.

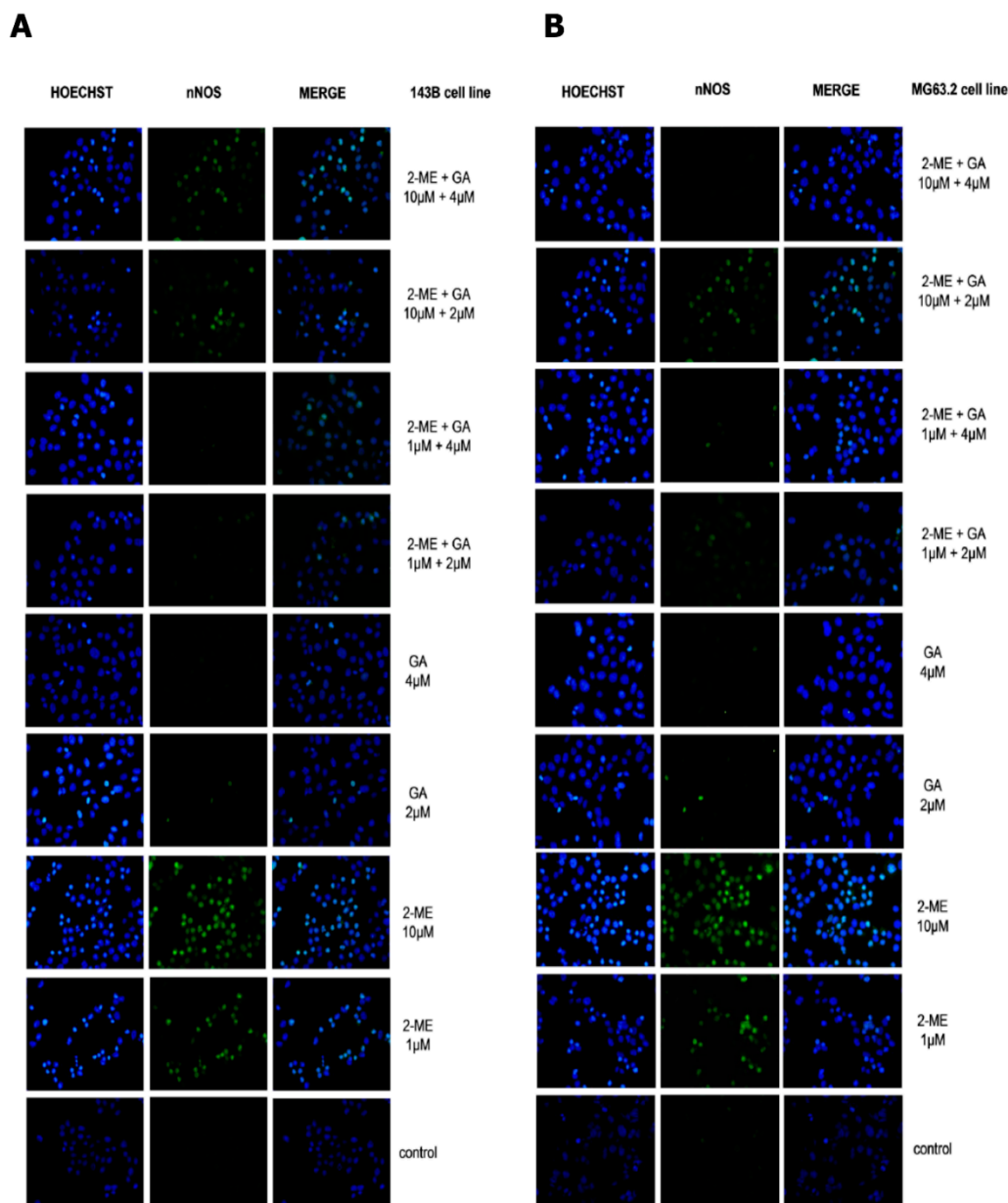


Figure 4. GA abrogates stimulatory effect of 2-ME on nNOS expression and nuclear translocation in 143B and MG63.2 cell lines. nNOS protein level in OS 143B and MG63.2 cells treated with vehiculum (Control) or either 2-ME or GA, or a combination of both compounds. OS 143B cells (**A**) and MG63.2 (**B**) were treated for with either 2-ME (1 µM or 10 µM) or GA (2 µM or 4 µM), or a combination of both for 8 h. The nNOS protein level was then determined by immunofluorescence. Cell nuclei were shown in blue, nNOS immunoreactivity in green, merged images of both in light blue. Original magnification $\times 40$. Each experiment was performed at least three times. The representative data are shown.

Notably, 1 µM and 10 µM 2-ME resulted in 1.5-, and 4-fold increase in the level of nNOS protein in 143B cells, while in 2.1 and 3.3-fold change in MG63.2 cells, respectively (Figure 2). GA alone did not significantly affect nNOS protein level. However, treatment with GA (2 µM or 4 µM) significantly abrogated 2-ME-induced nNOS protein after 8 h of incubation in comparison to 2-ME-treated cells (Figure 3).

Even more importantly, GA diminished the stimulatory effect of 2-ME on the nuclear translocation of nNOS as observed in the nuclear fractions of OS 143B cells (Figure 3C). All these obtained results, are supported by nNOS staining using immunofluorescence (Figure 4).

2.5. Nitro-Oxidative Stress Is Involved in the Interaction between 2-ME and GA in Osteosarcoma Cells

One of anticancer approach is a stimulation of generation of ROS and RNS [46–48]. Herein, we demonstrated that GA abrogates 2-ME-induced nuclear translocation nNOS what the most probably results in antagonistic interaction between the compounds.

Thus, next goal of the study was to determine the total pool of nitro-oxidative stress after combined or separated treatments of OS cells with 2-ME and GA depending on metastatic potential of OS cell line. MG63.2 and 143B cells were treated for 8 h with either 2-ME (1 μ M or 10 μ M) or GA (2 μ M or 4 μ M), or a combination of both (Figure 5).

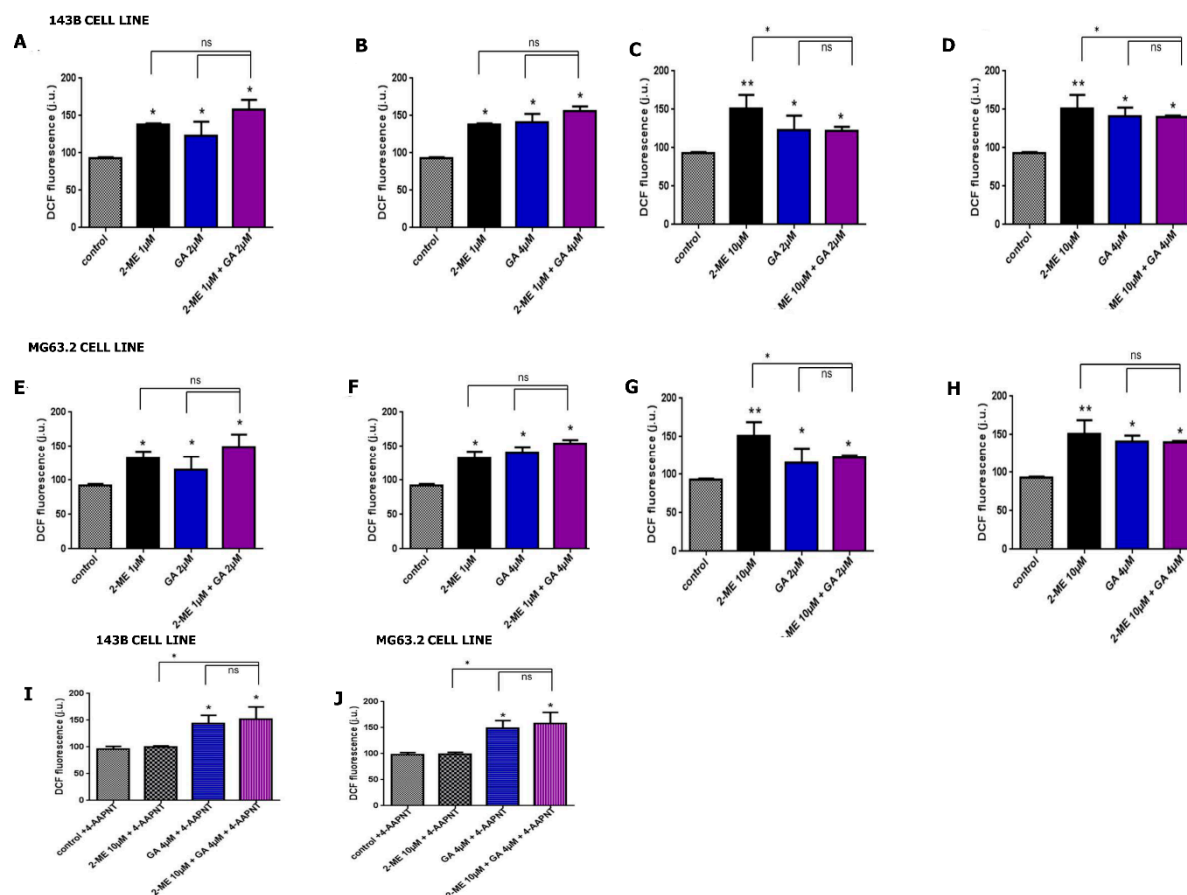


Figure 5. The total pool of nitro-oxidative stress in 143B (A–E) and MG63.2 cells (F–J) treated with either with 2-ME or GA, or a combination of both compounds. OS 143B cells (A–D,I) and MG63.2 (E–H,J) were treated for with vehiculum (Control) or either 2-ME (1 μ M or 10 μ M) or GA (2 μ M or 4 μ M), or a combination of both for 8 h. (I,J) present the data additionally using the pre-treatment with specific nNOS inhibitor (10 μ M 4-AAPNT) in OS 143B (I) and MG63.2 (J) cells. The total pool of nitro-oxidative stress was evaluated using 2',7'-dichlorofluorescein diacetate (DCF-DA) staining by means of flow cytometry. Data are presented as the mean \pm SE values form at least three independent experiments. The absence of error bar denotes a line thickness greater than the error. Data were analyzed by GraphPad Prism Software version 6.02 performing one way ANOVA analyses followed by Tukey's multiple comparison test. * $p < 0.01$, ** $p < 0.001$ versus control.

As demonstrated, both 2-ME (1 μ M or 10 μ M) and GA (2 μ M or 4 μ M), when used separately significantly increased pool of nitro-oxidative stress in 143B and MG63.2 cells after 8 h incubation (Figure 4). The nitro-oxidative stress levels in 143B and MG63.2 after 8 h long incubation with 2-ME or GA were comparable (Figure 5). While, incubation of 143B and MG63.2 cells with combination of 2-ME and GA for 8 h did not result in significant changes of the level of nitro-oxidative stress in comparison to the separate treatments (Figure 5). In addition to that, the level of ROS and RNS

generated after combined stimulation of 143B and MG63.2 cells with 10 μM 2-ME and 2 μM or 4 μM GA was diminished as compared to 2-ME used separately and the results were statistically significant (Figure 5).

To further elucidate the role of nNOS in the interaction between 2-ME and GA, we used the specific nNOS inhibitor, (*N*-[(4*S*)-4-amino-5-[(2-aminoethyl)amino]pentyl]-*N*-nitroguanidine tris(trifluoroacetate)) (4-AAPNT). Previously, we demonstrated that 2 h pre-treatment with 4-AAPNT inhibits 2-ME-induced nitro-oxidative stress [7,8]. As demonstrated, 2 h long pre-incubation of 143B and MG63.2 cells with a specific nNOS inhibitor, 10 μM 4-AAPNT, inhibited 2-ME-induced nitro-oxidative stress confirming that 2-ME-induced stress generation is mainly due to its impact on nNOS (Figure 5).

The nitro-oxidative stress level induced by the combined treatment with 2-ME (10 μM) and GA (4 μM) preceded by 4-AAPNT (10 μM) pre-incubation was at similar level in comparison to OS cells pretreated with 4-AAPNT (10 μM) and followed by treatment GA (4 μM) (Figure 5).

The obtained outcomes proposed the possible mechanism of lack of synergistic effects of 2-ME and GA that might be at least partially associated with their influence on nNOS activity and expression in OS cells.

2.6. Hsp90 Is Involved in the Interaction between 2-ME and GA in OS Cells

Due to the important role of Hsp90 as regulator of nNOS activity and expression [35–38], we further investigated whether Hsp90 is involved in 2-ME-induced induction and nuclear translocation of nNOS. Considering the consistency of the results obtained on 143B and MG63.2 cells, for further studies we chose 143B as a representative OS cell line.

OS 143B cells were treated with 2-ME (1 μM or 10 μM) or GA (2 μM or 4 μM), or the combination of both compounds for 8 h. Total Hsp90 (HSPC1), Hsp90 alpha (HSPC2), and Hsp90 beta (HSPC3) gene expression and protein level were then determined by means of Real Time PCR, Western blotting and immunofluorescence, respectively.

As demonstrated, 1 μM 2-ME had not impact on the level of Hsp90 alpha transcript (Figure 5). In contrast, treatment with 10 μM 2-ME resulted in significant upregulation of Hsp90 alpha gene expression by 6.7 fold (Figure 6). Treatment with both 2 μM and 4 μM GA increased Hsp90 alpha gene expression by 9.2 and 5 fold, respectively (Figure 6). Notably, the level of Hsp90 alpha transcript after combined treatment with 2-ME and GA was significantly downregulated in comparison to separate treatment with the compounds (Figure 6).

Consequently, we investigated impact of 2-ME and GA on the changes of Hsp90 beta gene expression. One micromole of 2-ME upregulated Hsp90 beta gene expression by 4.3-fold while 10 μM 2-ME did not impact on Hsp90 beta gene expression (Figure 6). Similarly to previously shown results for Hsp90 alpha, both 2 μM and 4 μM GA significantly increased the Hsp90 beta gene expression when used alone in comparison to the appropriate control by 3.9 and 3 fold, respectively. Notably, the level of Hsp90 beta gene expression after 8 h of combined treatment with 2-ME and GA was significantly diminished in comparison to cells separately treated with the compounds (Figure 6).

As demonstrated in Figure 6, the obtained results of the Hsp90 protein level are consistent with those obtained from Real Time PCR. Both 1 μM and 10 μM 2-ME increased the total Hsp90 protein expression by 1.8-, 1.3-fold, respectively (Figure 7A). The effect of GA on total Hsp90 protein level was concentration-dependent (Figure 7A). Treatment of 143B cells with 2 μM GA resulted in 60% decrease, while 4 μM GA 1.25-fold increase in the total Hsp90 protein level. Interestingly, the total level of Hsp90 protein after combined treatment of 143B with 2-ME (1 μM or 10 μM) and GA (2 μM or 4 μM) was significantly diminished (Figure 7A,B).

We further investigated whether the influence of 2-ME and GA on the total Hsp90 protein level was associated with their impact on Hsp90 alpha or Hsp90 beta. In consistency with Real Time PCR results, the 8 h of treatment of 143B cells with either 10 μM 2-ME or 4 μM GA, increased the level of Hsp90 alpha protein level by 3.2-, 5.5-fold, respectively as compared to control. While, the combined

treatment with the compounds resulted in a significant decrease in Hsp90 alpha protein level as compared to separate treatment with either 2-ME or GA alone (Figure 7C).

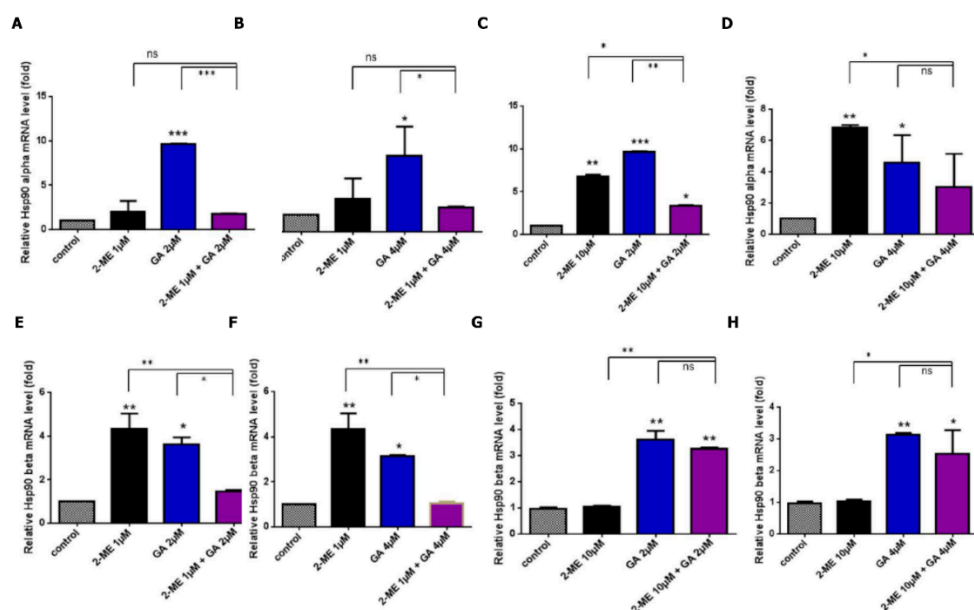


Figure 6. 2-ME and GA control the gene expression of Hsp90 alpha and Hsp90 beta in OS 143B cells. OS 143B cells were treated with either 2-ME (1 μM or 10 μM) or GA (2 μM or 4 μM) or in a combination of both for 8 h. Next, Hsp90 alpha (A–D) and Hsp90 beta (E–H) gene expression was determined by means of Real Time PCR. Data are presented as the mean ± SE values form at least three independent experiments. The absence of error bar denotes a line thickness greater than the error. Data were analyzed by GraphPad Prism Software version 6.02 performing one way ANOVA analyses followed by Tukey’s multiple comparison test. * $p < 0.01$, ** $p < 0.001$, *** $p < 0.0001$ versus control.

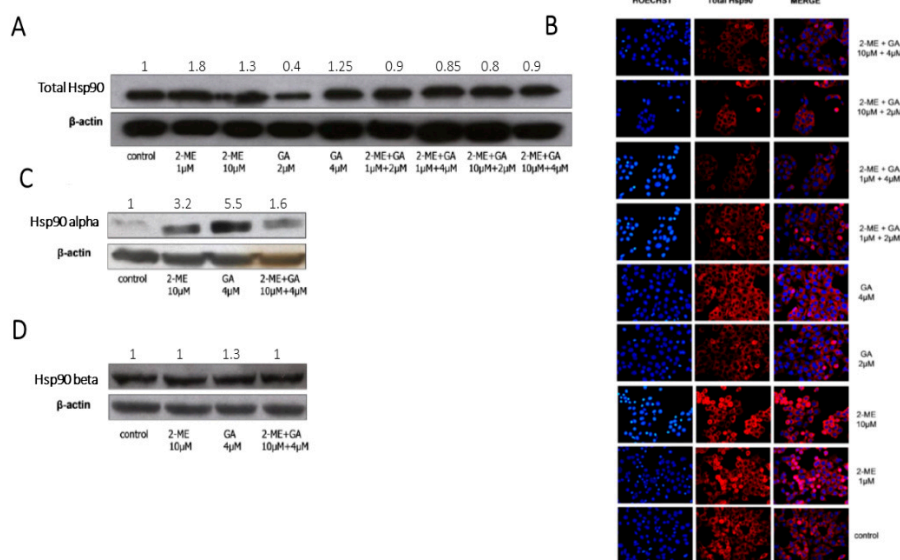


Figure 7. 2-ME and GA regulates the Hsp90 protein level in OS 143B cells. OS 143B cells were treated with vehiculum (Control), 2-ME (1 μM, 10 μM) or GA (2 μM, 4 μM) or combination of both for 8 h. Consequently, total pool of Hsp90 protein in OS 143B was determined by western blotting (A) and immunofluorescence (B), respectively. Cell nuclei were shown in blue, Hsp90 immunoreactivity in red, merged images of both in light red. Original magnification ×40. While the protein level of Hsp90 alpha (C) and Hsp90 beta (D) was evaluated by western blotting. Each experiment was performed at least three times. The representative data from three experiments are presented.

On the contrary, 8 h of treatment with 10 μM 2-ME did not impact on the Hsp90 beta protein level (Figure 7D). Treatment with 4 μM GA resulted in 30% increase in the Hsp90 beta protein level as compared to control. The combined treatment with 2-ME and GA did not impact on Hsp90 beta as compared to GA alone (Figure 7D).

2.7. Hsp70 Is Involved in the Interaction between 2-ME and GA in OS 143B Cells

Peng et al. evidenced that CHIP ligase requires Hsp70 for effective ubiquitination and proteasomal degradation of nNOS [36,37]. Therefore, our next goal of the study was to determine the changes of Hsp70 gene expression in OS 143B cells treated with either 2-ME (1 μM or 10 μM) or GA (2 μM or 4 μM), or a combination of both for 8 h.

As demonstrated, the separate 2-ME treatment did not influence Hsp70 gene expression in comparison to control (Figure 8A–D). On the other hand, treatment with 2 μM or 4 μM GA resulted in a dramatic upregulation of Hsp70 expression by 364- and 202.8-fold as compared to control, respectively (Figure 8A–D). The combined treatment with 1 μM 2-ME and 2 μM GA; 1 μM 2-ME and 4 μM GA; 10 μM 2-ME and 2 μM GA; 10 μM 2-ME and 4 μM GA resulted in an increase of the Hsp70 gene expression by 216-, 130-, 133-, and 138-fold as compared to control, respectively (Figure 8A–D). Nonetheless, the overexpression of Hsp70 gene induced by the combined treatment with 2-ME and GA was significantly diminished in comparison to the effect of GA when used separately (Figure 8A–D).

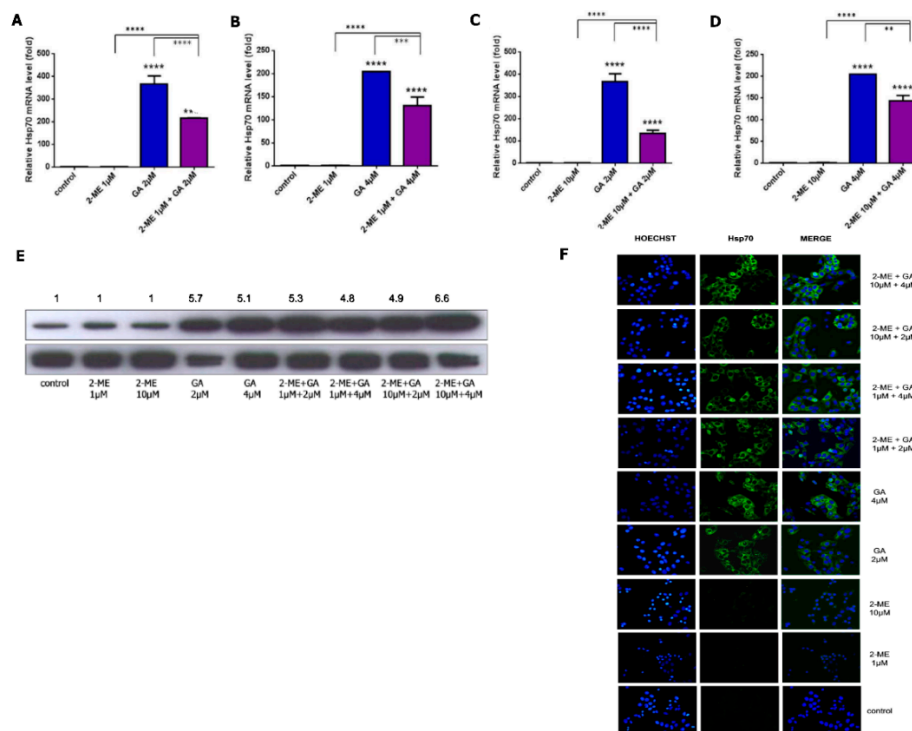


Figure 8. 2-ME has no effect on Hsp70, while GA controls the gene and protein expression of Hsp70 in OS 143B cells. OS 143B cells were treated with either 2-ME (1 μM or 10 μM) or GA (2 μM or 4 μM) or in a combination of both for 8 h. Next, Hsp70 (A–D) gene expression was determined by means of Real Time PCR. Consequently, total pool of Hsp70 protein in OS 143B was determined by western blotting (E) and immunofluorescence (F), respectively. Cell nuclei were shown in blue, Hsp70 immunoreactivity in green, merged images of both in light green. Original magnification $\times 40$. The representative data from three experiments are presented. Data are presented as the mean \pm SE values form at least three independent experiments. The absence of error bar denotes a line thickness greater than the error. Data were analyzed by GraphPad Prism Software version 6.02 performing one way ANOVA analyses followed by Tukey’s multiple comparison test. ** $p < 0.001$, *** $p < 0.0001$, **** $p < 0.00001$ versus control.

We further investigated the impact of the tested compounds on the Hsp70 (HSPA1) cellular protein level by western blotting and immunofluorescence (Figure 8E,F). As demonstrated, the obtained results of Hsp70 protein level were consistent with the results from Real Time PCR. 2-ME did not impact on Hsp70 protein expression in comparison to control (Figure 8E,F). On the other hand, GA upregulated Hsp70 protein level in a concentration-dependent manner as compared to control (Figure 8E,F). Quantitative analyses revealed 5.7- and 5.1-fold upregulation of Hsp70 protein by 2 μ M, and 4 μ M GA, respectively (Figure 8E).

3. Discussion

2-ME is a powerful anticancer agent that may be used in treatment of great number of malignancies, including OS [4–19]. While there are few studies on GA-induced OS cell death [41,49–51]. Notably, the analog of GA; 17-N-Allylamino-17-demethoxygeldanamycin, was evaluated in phase I study in pediatric patients with recurrent or refractory solid tumors, including OS [51].

In the present study we observed the antagonistic effect between 2-ME and GA in employed OS cell death model. A closer look into the mechanism of action of these two compounds revealed new insight into nNOS as potential target of both 2-ME and GA. In our previous studies we showed that 2-ME drives nNOS nuclear hijacking and therefore local generation of nitric oxide leading to DNA damage [10] and/or inhibition of mitochondrial biogenesis [4–8] in OS 143B cellular model. Herein, the results were supported by using highly metastatic OS MG63.2 cell line [42,43].

Nuclear localization of nNOS upon activity of 2-ME is specifically interesting in light of the fact that nNOS is believed to be essentially a cytosolic isoform [32,52,53]. While, the enzyme may be translocated into nucleus under specific conditions [29,54,55].

Notably, in the present study we evidenced that GA, being a potent inhibitor of Hsp90, decreases 2-ME-mediated induction and nuclear translocation of nNOS independently on metastatic potential of OS cells. Up to date, there have been no data concerning the impact of GA on the modulation of activity or expression of nNOS. While, GA is believed to interfere with eNOS and iNOS [56,57]. species. Mechanisms underlying on the regulation of the activity and expression of NOS are complex and may be regulated by different factors including Hsps. It is well known that nNOS is a Hsp90-client protein [36,58–60]. Isoforms of NOS tend to assemble hetero-complexes with Hsp90 being promptly disassembled (dynamic cycling, “hit and run”) [61]. Hsp90 is believed to directly enhance synthesis of nitric oxide catalyzed by nNOS, which is partially dependent on the enhancement of calmodulin binding to nNOS [58–63]. Moreover, Hsp90 is also required for heme binding and for the formation of catalytically active nNOS [62,63].

Two major cytoplasmic isoforms of Hsp90, inducible form Hsp90 alpha and constitutively expressed Hsp90 beta can be distinguished [64]. As evidenced here, 2-ME in a concentration-dependent manner upregulated both the inducible Hsp90 alpha and constitutively expressed Hsp90 beta in OS cell death model. Currently, there are no studies concerning impact of different Hsp90 isoforms on activity of nNOS. As suggested by Chao et al., it could be due to specific SDS-PAGE conditions [65].

Therefore, herein, for the first time, a role of Hsp90 alpha in the regulation of nNOS protein level and nuclear localization of the enzyme was investigated. The effect of Hsp90 beta on iNOS activity was previously reported [66]. However, this model highlighted apoptosis of human chondrocytes and might not necessarily correspond our OS cell death model [66]. On the other hand, 2-ME was reported to increase the level of Hsp90 alpha transcripts in breast cancer MCF-7 cell line [67]. However, the detailed mechanism and specifically transcription factors involved in 2-ME-induced Hsp90 gene expression have not been revealed. Previously, Hsp90 alpha has been related to the formation of the so called “apoptotic ring” and the activation of nuclear apoptosis execution [68]. An observation of increased protein level of Hsp90 alpha caused by 2-ME can support the hypothesis that a nuclear localization of 2-ME-induced nNOS is associated with apoptosis of OS cells.

Herein, we presented that GA has a remarkable capability of reversing 2-ME-mediated induction of nNOS and nuclear hijacking of the enzyme. Though, the mechanism of cytoplasm-nuclear shuttle

of nNOS is not fully understood, we propose that Hsp90 takes part in enzyme nuclear translocation. Indeed, nuclear translocation of the phosphoprotein Hop (Hsp70/Hsp90 organizing protein) was established to occur under heat shock and directly associated with Hsp90 binding [69]. On the other hand, there is evidence that nascent steroid receptors form an oligomeric complex in the cytoplasm with Hsp90, Hsp70, and some other proteins, and dissociation of Hsp90 from the complex is prerequisite for the nuclear transport of the receptors [70].

Indeed, GA was previously reported to impact HSP expression by stabilization of the transcription factor HSF1 trimeric complex with HSE, and thus stimulating the induction of HSP coding genes [71]. Here, we presented that GA modulated Hsp90 gene and protein expressions in a dose-dependent manner. As we have proved, increased Hsp90 protein expression is associated mainly with the impact of GA on Hsp90 alpha, which correlates with its inducible potential [64]. In addition to that, a dose-dependent effect of GA regulating Hsp90 expression has been recently demonstrated by Karkoulis et al. [72]. The higher induction of gene expression caused by 2 μ M GA as opposed to 4 μ M GA, and surprisingly enough, a decreased protein level observed after stimulation with 2 μ M GA, can be explained by compensation mechanisms and/or different mRNA stability regulation. Notably, GA abrogated also 2-ME -induced upregulation of Hsp90 protein level which is in correlation with decreased expression of nNOS and inhibition of its nuclear localization in employed OS cellular model.

In the case when Hsp90 does no longer chaperone the nNOS, E3 ligase interacts with Hsp70 in order to initiate protein degradation [35–37]. Hsp70 possesses the same binding site within the oxygenase domain of nNOS as Hsp90 [36]. In light of these facts, the overexpression of Hsp70 in contrast to Hsp90, promotes ubiquitination and proteasomal degradation of nNOS [36,37]. Thus, we associate decreased level of nNOS protein after a combined treatment with 2-ME and GA or with GA with the accompanying upregulation of Hsp70 and further proteasomal degradation of nNOS.

The obtained overexpression of Hsp70 after treatment with GA is also important from clinical point of view. Importantly, 2-ME used separately did not affect Hsp70 expression. In a number of cancers such as OS, an increased level of Hsp70, relative to the Hsp70 level in non-transformed cells was clinically confirmed [73–76]. Inhibition of Hsp70 sensitizes cancer cells to apoptosis [36], therefore is also linked with better outcome of chemotherapy [76]. Thus, observed in the present study upregulation of Hsp70 by GA may be suggested as one of the main mechanisms leading to the development of chemo-resistance [77].

All the obtained data were in consistency with pool of nitro-oxidative stress after treatment with the compounds. Indeed, although GA cytotoxicity has been attributed to its disruption of Hsp90 complexes, this compound also carries a benzoquinone moiety that generates reactive oxygen species [78,79].

4. Materials and Methods

4.1. Reagents

Tissue culture media, antibiotic cocktail, heat inactivated fetal bovine serum and 2-methoxyestradiol were purchased from Sigma–Aldrich (Soborg, Denmark). The list of the primary antibodies used in the current study is given in a Table 2 below.

In order to clarify the type of investigated Hsps, we presented the list of used antibodies, indicating the name of protein including old and new nomenclature suggested by Kampinga et al., 2008 [80] (Table 2).

Table 2. The list of primary antibodies used in the current study.

Protein	Clonality	Clone Number	Catalog Number	Company
Hsp90 HSPC1	monoclonal	4F10	sc-69703	Santa Cruz Biotechnology, Inc. (Heidelberg, Germany)
HSP90 alpha HSPC2	polyclonal	-	ab2928	Abcam (Cambridge, UK)
Hsp90 beta HSPC3	polyclonal	-	ab80159	Abcam (Cambridge, UK)
HSP70 HSP70-1/HSP70-2 HSPA1 HSPA1A/1B	monoclonal	EP1007Y	ab45133	Abcam (Cambridge, UK)
HSP60 GROEL HSPD1	monoclonal	H1	sc-13115	Santa Cruz Biotechnology, Inc. (Heidelberg, Germany)
nNOS NOS type I	monoclonal	16/nNOS/NOS Type I	610309	BD Biosciences (San Jose, CA, USA)
Beta actin	monoclonal	C4	sc-47778	Santa Cruz Biotechnology, Inc. (Heidelberg, Germany)

4.2. Cell Line and Culture Conditions

The human osteosarcoma 143B cell line (ATTC-8303) was purchased from Sigma–Aldrich (Soborg, Denmark). Highly metastatic human osteosarcoma MG63.2 cell line [42–44] was established by prof. Hue H. Luu from Department of Surgery, Orthopedic Surgery, Orthopedic Oncology and Adult Reconstruction Associate Director, Molecular Oncology Laboratory, The University of Chicago, USA.

The cells were cultured at 37 °C in a humidified atmosphere saturated with 5% CO₂. The cells were maintained in monolayer culture using EMEM supplemented with 10% heat inactivated FBS, 2 mL-glutamine, penicillin (100 U/mL)/streptomycin (100 µg/mL) cocktail. For cellular treatment, the medium supplemented only with 1% charcoal FBS was used. In order to avoid the impact of the solvents, control cells were treated with an equal volume of the solvent used to prepare 2-ME and GA solutions.

4.3. Cell Viability Assay (MTT Assay)

OS 143B and MG63.2 cells were treated with serial dilutions of 2-ME, GA or their combination (molar ratio 1:1) (within the concentration range of 0.8–50 µM) of 2-ME for 24 h. The MTT assay was performed as previously described [4–8]. The results are presented as a percentage of control. Each experiment was performed at least three times.

4.4. Drug Dose–Effect Calculations and Analysis of Interaction Using CalcuSyn Software (Biosoft)

The CalcuSyn analysis (CalcuSyn, version 2.11, Biosoft, Cambridge, UK) was performed as previously described [45] and as indicated in manufacturer’s protocole. The software uses the Median-effect equation:

$$f_a/f_u = (D/D_m)^m$$

where:

D: the dose of drug

D_m: the median-effect dose signifying the potency

f_a: the fraction affected by the dose

f_u : the fraction unaffected, where $f_u = 1 - f_a$

m : an exponent signifying the sigmoidicity (shape) of the dose effect curve

The median-effect plot: A plot of $x = \log(D)$ vs $y = \log(f_a/f_u)$.

D_m value: the median-effect dose or concentration.

m value: a measurement of the sigmoidicity of the dose–effect curve; $m = 1$, >1 , and <1 indicates hyperbolic, sigmoidal, and negative sigmoidal shape, respectively.

r value: The linear correlation coefficient of the median-effect plot.

Combination index (CI): A quantitative measure of the degree of drug interaction in terms of additive effect (CI = 1), synergism (CI < 1), or antagonism (CI > 1) for a given endpoint of the effect measurement.

4.5. Analysis of Apoptosis and Necrosis by Flow Cytometry

Rate of apoptotic and necrotic cells was analyzed by means of flow cytometry as previously described [8]. Briefly, 143B and MG63.2 cells were seeded in 6-well plates at a density of 300,000 cells per well. After 24 h, the cells were treated with 2-ME and GA separately or in combination for 24 h. The cells were then trypsinased and harvested. Afterwards, the samples were incubated with Annexin V and propidium iodide (PI) for 15 min at room temperature. The cells were then counted at 30,000, and the fluorescence signals of Annexin V and PI conjugate were detected in the fluorescence intensity channels FL1 and FL3 (BD FACScan, Becton-Dickinson, Franklin Lakes, NJ, USA). The obtained were analyzed using Cyflog software, version 1.2.1 (CyFlo Ltd., Turku, Finland). The procedure was repeated at least 3 times to ensure repeatability of results.

4.6. Detection of Nitro-Oxidative Stress by Flow Cytometry

Reactive oxygen and nitrogen species [46] were determined using flow cytometry with 2',7'-dichlorofluorescein diacetate (DCF-DA) staining as previously described [4–8]. Briefly, the cells were seeded onto six-well plates at a density of 300,000 cells/ well. After 24 h of culturing in the normal growth medium, cells were exposed to treatment with 2-ME and/or GA. DCF-DA at final concentration of 10 μ M was added to the cell medium 30 min before end of incubation. Afterward, 30,000 cells were analyzed by flow cytometry (BD FACScan, Becton-Dickinson, Franklin Lakes, NJ, USA) and the results were analyzed by Cyflog software, version 1.2.1 (CyFlo Ltd., Turku, Finland). Each experiment was performed at least three times to ensure repeatability of results.

4.7. Western Blotting

Equal amounts of total cell lysates were resolved by 7% and 12% SDS-PAGE for nNOS and Hsps analyses, respectively. The membranes were then incubated with primary antibodies anti-nNOS (dilution 1:1000), anti-Hsp90, Hsp90 alpha, Hsp90 beta, Hsp70, Hsp60 (Table 1) (dilution 1:5000) overnight at 4 °C and next, analysis performed as previously described [4–8,81]. The cytoplasmic and nuclear fractions were separated using the Nuclear Extract Kit (Active Motif, France) according to manufacturer's protocol. The protein level was quantified by densitometry technique using the Quantity one 4.5.2 software (Bio-Rad, Feldkirchen, Germany). The protein levels, as determined by chemiluminescent quantification, were normalized relative to beta-actin levels (dilution 1:50,000). Each experiment was performed at least three times.

4.8. RNA Extraction and Real Time PCR Analyses

The real time PCR analyses were performed as previously described [9]. Briefly, RNA was extracted using a Total RNA Mini Plus kit (A&A Biotechnology, Gdynia, Poland) according to the manufacturer's protocol. The concentration and purity of isolated RNA were measured with an Epoch spectrophotometer (BioTek, Winooski, VT, USA). Two micrograms of total RNA were reverse transcribed into cDNA with RevertAid™ First Strand cDNA Synthesis kit according to the

manufacturer's instructions (Thermo Fisher Scientific Inc., USA.). The Real-Time PCR reactions were performed in duplicates with Real-Time HS 2× PCR Master Mix SYBR[®] kit (A&A Biotechnology, Gdynia, Poland). The PCR conditions were: 95 °C for 10 min followed by 40 cycles of denaturation for 15 s at 95 °C, annealing for 15 s at 60 °C, extension for 15 s at 72 °C, and fluorescence reading for 10 s at 79 °C. Dynamic melting curve analysis was performed for all reactions. The data were collected using the StepOnePlus™ Real-Time PCR System (Life Technologies-Applied Biosystems, Grand Island, NY, USA). Primers were optimized for RT-PCR target gene expression, which was normalized against the housekeeping gene, *RPL37*. Statistically significant differences between treated and control cell lines were determined using comparative delta-delta Ct test. The primer sequences used in the study are given in Table 3 below.

Table 3. Primer sequences used in the study.

Gene	Forward Primer (5'-3')	Reverse Primer (5'-3')
<i>HSP90AA1 (ALPHA)</i>	AGGTTGAGACGTTTCGCCTTTCA	AGATATCTGCACCAGCCTGCAA
<i>HSP90AB1 (BETA)</i>	AGGAACGTACCCTGACTTTGGT	ATGCCAATGCCTGTGTCTACCA
<i>HSP70</i>	AAGGACATCAGCCAGAACAAGCGA	ACGTGTAGAAGTCGATGCCCTCAA
<i>RPL37</i>	TTCTGATGGCGGACTTTACC	CACTTGCTCTTTCTGTGGCA

4.9. Immunofluorescence Microscopy

The immunofluorescence was performed as previously described [10]. Briefly, the cells were treated with 2-ME and/or GA. Anti-nNOS, Hsp90, Hsp70, Hsp60 (1:50 in 0.3% GSA, 2 h incubation) (Table 1) and secondary-conjugated with CY3 (1:100, GAM Cy3, 1 h incubation, Jackson ImmunoResearch, Suffolk, UK) antibodies were used. The images were analyzed and merged employing the ImageJ software 1.44p. Each experiment was performed at least three times

4.10. Statistical Analysis

Data are presented as the mean ± SE values from at least three independent experiments. Data were analyzed using GraphPad Prism (GraphPad Software, Inc., version 6.03, La Jolla, CA, USA). Significant differences between groups were determined by One-way ANOVA combined with Tuckey's Multiple Comparison test.

5. Conclusions

Herein, we evidenced that inhibition of Hsp90 by GA controls the protein expression of 2-ME-induced nNOS and inhibits enzyme nuclear translocation. Based on the obtained results, we propose that decreased level of nNOS after a combined treatment with 2-ME and GA is directly associated with the accompanying upregulation of Hsp70 and downregulation of Hsp90. This interaction resulted in abrogation of anticancer efficacy of 2-ME by GA.

Because of at least partly contradictory signaling pathways in OS cell death model, 2-ME and GA should not be used in combination for cancer therapy even if the outcome of clinical trials is successful for either one alone.

Author Contributions: Conceptualization M.G.-P.; methodology M.G.-P., A.K.-J., A.M.-G., A.D., J.M.W., M.A.Z., F.C.; data analysis M.G.-P.; investigation M.G.-P.; data curation M.G.-P.; writing—original draft preparation M.G.-P.; writing—review and editing M.G.-P., A.K.-J., A.M.G., A.D., J.M.W., M.A.Z., H.H.L., M.W., F.C.; visualization M.G.-P.; supervision M.G.-P.; project administration M.G.-P.; funding acquisition M.G.-P. All authors have read and agreed to the published version of the manuscript.

Funding: The part of the studies concerning anticancer mechanism of action of 2-methoxyestradiol as well as publication of the manuscript were funded by the Iuventus Plus project of Polish Ministry of Science and Higher Education No IP 2015 022074. The funders had no role in study design, data collection and analysis, decision to publish, or preparation of the article.

Acknowledgments: M.W. kindly acknowledges support from ST46 funds provided by Medical University of Gdansk (Poland). A.M.G. and F.C. kindly acknowledge support from the project “GeSeTon”, Management of an integrated multicentric service of diagnostics and customized therapy in oncology” funded by Ministry of Economic Development by E.U. indirect funds (PON-GRANDI PROGETTI R&S, 2014/2020). Magdalena Gorska-Ponikowska kindly acknowledges being a guest scientist in the prof. Stephan Nussberger lab at Stuttgart University (Stuttgart, Germany); and in the prof. Francesco Cappello lab at Euro-Mediterranean Institute of Science and Technology (Palermo, Italy).

Conflicts of Interest: The authors declare no conflict of interest.

Data Availability: The data used to support the findings of this study are available from the corresponding author upon request.

References

1. Biazzo, A.; De Paolis, M. Multidisciplinary approach to osteosarcoma. *Acta Orthop. Belg.* **2016**, *82*, 690–698. [[PubMed](#)]
2. Kager, L.; Tamamyan, G.; Bielack, S. Novel insights and therapeutic interventions for pediatric osteosarcoma. *Future Oncol.* **2016**, *13*, 357–368. [[CrossRef](#)] [[PubMed](#)]
3. Kansara, M.; Teng, M.W.; Smyth, M.J.; Thomas, D.M. Translational biology of osteosarcoma. *Nat. Rev. Cancer* **2014**, *14*, 722–735. [[CrossRef](#)] [[PubMed](#)]
4. Gorska-Ponikowska, M.; Kuban-Jankowska, A.; Eisler, S.A.; Perricone, U.; Lo Bosco, G.; Barone, G.; Nussberger, S. 2-methoxyestradiol affects mitochondrial biogenesis pathway and succinate dehydrogenase complex flavoprotein subunit A in osteosarcoma cancer cells. *Cancer Genom. Proteom.* **2018**, *15*, 73–89.
5. Gorska-Ponikowska, M.; Kuban-Jankowska, A.; Daca, A.; Nussberger, S. 2-methoxyestradiol reverses the pro-carcinogenic effect of L-lactate in osteosarcoma 143B cells. *Cancer Genom. Proteom.* **2017**, *14*, 483–493.
6. Gorska, M.; Kuban-Jankowska, A.; Milczarek, R.; Wozniak, M. Nitro-oxidative stress is involved in anticancer activity of 17 β -estradiol derivative in neuroblastoma cells. *Anticancer Res.* **2016**, *36*, 1693–1698.
7. Gorska, M.; Kuban-Jankowska, A.; Zmijewski, M.; Gammazza, A.M.; Cappello, F.; Wnuk, M.; Gorzynik, M.; Rzesutek, I.; Daca, A.; Lewinska, A.; et al. DNA strand breaks induced by nuclear hijacking of neuronal NOS as an anti-cancer effect of 2-methoxyestradiol. *Oncotarget* **2015**, *6*, 15449–15463. [[CrossRef](#)]
8. Gorska, M.; Kuban-Jankowska, A.; Zmijewski, M.A.; Gorzynik, M.; Szkatula, M.; Wozniak, M. Neuronal nitric oxide synthase induction in the antitumorigenic and neurotoxic effects of 2-methoxyestradiol. *Molecules* **2014**, *19*, 13267–13281. [[CrossRef](#)]
9. Gorska, M.; Kuban-Jankowska, A.; Antoniewicz, J.; Wozniak, M. Effect of 2-methoxyestradiol on dephosphorylation of neuronal nitric oxide synthase in osteosarcoma 143B cells. An in vitro study. *J. Clin. Toxicol.* **2015**, *5*, 1–4. [[CrossRef](#)]
10. Bruce, J.Y.; Eickhoff, J.; Pili, R.; Logan, T.; Carducci, M.; Arnott, J.; Treston, A.; Wilding, G.; Liu, G. A phase II study of 2-methoxyestradiol nanocrystal colloidal dispersion alone and in combination with sunitinib malate in patients with metastatic renal cell carcinoma progressing on sunitinib malate. *Investig. New Drugs* **2012**, *30*, 794–802. [[CrossRef](#)]
11. Kulke, M.H.; Chan, J.A.; Meyerhardt, J.A.; Zhu, A.X.; Abrams, T.A.; Blaszkowsky, L.S.; Regan, E.; Sidor, C.; Fuchs, C.S. A prospective phase II study of 2-methoxyestradiol administered in combination with bevacizumab in patients with metastatic carcinoid tumors. *Cancer Chemother. Pharmacol.* **2011**, *68*, 293–300. [[CrossRef](#)] [[PubMed](#)]
12. Harrison, M.R.; Hahn, N.M.; Pili, R.; Oh, W.K.; Hammers, H.; Sweeney, C.; Kim, K.; Perlman, S.; Arnott, J.; Sidor, C.; et al. A phase II study of 2-methoxyestradiol (2ME2) NanoCrystal[®] dispersion (NCD) in patients with taxane-refractory, metastatic castrate-resistant prostate cancer (CRPC). *Investig. New Drugs* **2011**, *29*, 1465–1474. [[CrossRef](#)]
13. Matei, D.; Schilder, J.; Sutton, G.; Perkins, S.; Breen, T.; Quon, C.; Sidor, C. Activity of 2 methoxyestradiol (Panzem NCD) in advanced, platinum-resistant ovarian cancer and primary peritoneal carcinomatosis: A Hoosier Oncology Group trial. *Gynecol. Oncol.* **2009**, *115*, 90–96. [[CrossRef](#)] [[PubMed](#)]
14. Tevaarwerk, A.J.; Holen, K.D.; Alberti, D.B.; Sidor, C.; Arnott, J.; Quon, C.; Wilding, G.; Liu, G. Phase I trial of 2-methoxyestradiol NanoCrystal dispersion in advanced solid malignancies. *Clin. Cancer Res.* **2009**, *15*, 1460–1465. [[CrossRef](#)] [[PubMed](#)]

15. James, J.; Murry, D.J.; Treston, A.M.; Storniolo, A.M.; Sledge, G.W.; Sidor, C.; Miller, K.D. Phase I safety, pharmacokinetic and pharmacodynamic studies of 2-methoxyestradiol alone or in combination with docetaxel in patients with locally recurrent or metastatic breast cancer. *Investig. New Drugs* **2007**, *25*, 41–48. [[CrossRef](#)]
16. Dahut, W.L.; Lakhani, N.J.; Gulley, J.L.; Arlen, P.M.; Kohn, E.C.; Kotz, H.; McNally, D.; Parr, A.; Nguyen, D.; Yang, S.X.; et al. Phase I clinical trial of oral 2-methoxyestradiol, an antiangiogenic and apoptotic agent, in patients with solid tumors. *Cancer Biol. Ther.* **2006**, *5*, 22–27. [[CrossRef](#)]
17. Tomillero, A.; Moral, M.A. Gateways to clinical trials. *Methods Find. Exp. Clin. Pharmacol.* **2009**, *31*, 661–700. [[CrossRef](#)]
18. Zhou, Q.; Gustafson, D.; Nallapareddy, S.; Diab, S.; Leong, S.; Lewis, K.; Gore, L.; Messersmith, W.A.; Treston, A.M.; Eckhardt, S.G.; et al. A phase I dose-escalation, safety and pharmacokinetic study of the 2-methoxyestradiol analog ENMD-1198 administered orally to patients with advanced cancer. *Investig. New Drugs* **2011**, *29*, 340–346. [[CrossRef](#)]
19. Sweeney, C.; Liu, G.; Yiannoutsos, C.; Kolesar, J.; Horvath, D.; Staab, M.J.; Fife, K.; Armstrong, V.; Treston, A.; Sidor, C.; et al. A phase II multicenter, randomized, double-blind, safety trial assessing the pharmacokinetics, pharmacodynamics, and efficacy of oral 2-methoxyestradiol capsules in hormone-refractory prostate cancer. *Clin. Cancer Res.* **2005**, *11*, 6625–6633. [[CrossRef](#)]
20. Kamath, K.; Okouneva, T.; Larson, G.; Panda, D.; Wilson, L.; Jordan, M.A. 2-Methoxyestradiol suppresses microtubule dynamics and arrests mitosis without depolymerizing microtubules. *Mol. Cancer Ther.* **2006**, *5*, 2225–2233. [[CrossRef](#)]
21. Ricker, J.L.; Chen, Z.; Yang, X.P.; Pribluda, V.S.; Swartz, G.M.; Van Waes, C. 2-methoxyestradiol inhibits hypoxia-inducible factor 1alpha, tumor growth, and angiogenesis and augments paclitaxel efficacy in head and neck squamous cell carcinoma. *Clin. Cancer Res.* **2004**, *10*, 8665–8673. [[CrossRef](#)] [[PubMed](#)]
22. Mooberry, S.L. New insights into 2-methoxyestradiol, a promising antiangiogenic and antitumor agent. *Curr. Opin. Oncol.* **2003**, *15*, 425–430. [[CrossRef](#)] [[PubMed](#)]
23. LaVallee, T.M.; Zhan, X.H.; Herbstritt, C.J.; Kough, E.C.; Green, S.J.; Pribluda, V.S. 2-Methoxyestradiol inhibits proliferation and induces apoptosis independently of estrogen receptors alpha and beta. *Cancer Res.* **2002**, *62*, 3691–3697.
24. Pribluda, V.S.; Gubish, E.R., Jr.; Lavalley, T.M.; Treston, A.; Swartz, G.M.; Green, S.J. 2-Methoxyestradiol: An endogenous antiangiogenic and antiproliferative drug candidate. *Cancer Metastasis Rev.* **2000**, *19*, 173–179. [[CrossRef](#)] [[PubMed](#)]
25. Fotsis, T.; Zhang, Y.; Pepper, M.S.; Adlercreutz, H.; Montesano, R.; Nawroth, P.P.; Schweigerer, L. The endogenous oestrogen metabolite 2-methoxyoestradiol inhibits angiogenesis and suppresses tumour growth. *Nature* **1994**, *368*, 237–239. [[CrossRef](#)] [[PubMed](#)]
26. Mueck, A.O.; Seeger, H. 2-Methoxyestradiol-Biology and mechanism of action. *Steroids* **2010**, *75*, 625–631. [[CrossRef](#)]
27. Seegers, J.C.; Lottering, M.L.; Grobler, C.J.; Van Papendorp, D.H.; Habbersett, R.C.; Shou, Y.; Lehnert, B.E. The mammalian metabolite, 2-methoxyestradiol, affects p53 levels and apoptosis induction in transformed cells but not in normal cells. *J. Steroid Biochem. Mol. Biol.* **1997**, *62*, 253–267. [[CrossRef](#)]
28. Foerstermann, U.; Sessa, W.C. Nitric oxide synthases: Regulation and function. *Eur. Heart J.* **2012**, *33*, 829–837. [[CrossRef](#)]
29. Zhou, L.; Zhu, D.-Y. Neuronal nitric oxide synthase: Structure, subcellular localization, regulation, and clinical implications. *Nitric Oxide Biol. Chem.* **2009**, *20*, 223–230. [[CrossRef](#)]
30. Nakane, M.; Gehrke, L.; Schmidt, H.; Pollock, J.S.; Forstermann, U. Cloned human brain nitric-oxide synthase is highly expressed in skeletal muscle. *FASEB J.* **1993**, *7*, A258. [[CrossRef](#)]
31. Wang, Y.; Marsden, P.A. Nitric oxide synthases: Gene structure and regulation. *Adv. Pharmacol.* **1995**, *34*, 71–90. [[PubMed](#)]
32. Zhang, Y.H.; Casadei, B. Sub-cellular targeting of constitutive NOS in health and disease. *J. Mol. Cell. Cardiol.* **2012**, *52*, 341–350. [[CrossRef](#)] [[PubMed](#)]
33. Gorska, M.; Zmijewski, M.A.; Kuban-Jankowska, A.; Wnuk, M.; Rzeszutek, I.; Wozniak, M. Neuronal nitric oxide synthase-mediated genotoxicity of 2-methoxyestradiol in hippocampal HT22 cell line. *Mol. Neurobiol.* **2016**, *53*, 5030–5040. [[CrossRef](#)] [[PubMed](#)]
34. Su, Y. Regulation of endothelial nitric oxide synthase activity by protein-protein interaction. *Curr. Pharm. Des.* **2014**, *20*, 3514–3520. [[CrossRef](#)]

35. García-Cardena, G.; Fan, R.; Shah, V.; Sorrentino, R.; Cirino, G.; Papapetropoulos, A.; Sessa, W.C. Dynamic activation of endothelial nitric oxide synthase by Hsp90. *Nature* **1998**, *392*, 821–824. [[CrossRef](#)]
36. Bender, A.T.; Silverstein, A.M.; Demady, D.R.; Kanelakis, K.C.; Noguchi, S.; Pratt, W.B.; Osawa, Y. Neuronal nitric-oxide synthase is regulated by the Hsp90-based chaperone system in vivo. *J. Biol. Chem.* **1999**, *274*, 1472–1478. [[CrossRef](#)]
37. Peng, H.M.; Morishima, Y.; Clapp, K.M.; Lau, M.; Pratt, W.B.; Osawa, Y. Dynamic cycling with Hsp90 stabilizes neuronal nitric oxide synthase through calmodulin-dependent inhibition of ubiquitination. *Biochemistry* **2009**, *48*, 8483–8490. [[CrossRef](#)]
38. Peng, H.M.; Morishima, Y.; Pratt, W.B.; Osawa, Y. Modulation of heme/substrate binding cleft of neuronal nitric-oxide synthase (nNOS) regulates binding of Hsp90 and Hsp70 proteins and nNOS ubiquitination. *J. Biol. Chem.* **2012**, *287*, 1556–1565. [[CrossRef](#)]
39. Clapp, K.M.; Peng, H.M.; Jenkins, G.J.; Ford, M.J.; Morishima, Y.; Lau, M.; Osawa, Y. Ubiquitination of neuronal nitric-oxide synthase in the calmodulin-binding site triggers proteasomal degradation of the protein. *J. Biol. Chem.* **2012**, *287*, 42601–42610. [[CrossRef](#)]
40. Chan, J.Y.H.; Cheng, H.L.; Chou, J.L.; Li, F.C.; Dai, K.Y.; Chan, S.H.; Chang, A.Y. Heat shock protein 60 or 70 activates nitric-oxide synthase (NOS) I-and inhibits NOSII-associated signaling and depresses the mitochondrial apoptotic cascade during brain stem death. *J. Biol. Chem.* **2007**, *282*, 4585–4600. [[CrossRef](#)]
41. Franke, J.; Eichner, S.; Zeilinger, C.; Kirschning, A. Targeting heat-shock-protein 90 (Hsp90) by natural products: Geldanamycin, a show case in cancer therapy. *Nat. Prod. Rep.* **2013**, *30*, 1299–1323. [[CrossRef](#)] [[PubMed](#)]
42. Su, Y.; Wagner, E.R.; Luo, Q.; Huang, J.; Chen, L.; He, B.C.; Zuo, G.W.; Shi, Q.; Zhang, B.Q.; Zhu, G.; et al. Insulin-like growth factor binding protein 5 suppresses tumor growth and metastasis of human osteosarcoma. *Oncogene* **2011**, *30*, 3907–3917. [[CrossRef](#)] [[PubMed](#)]
43. Su, Y.; Luo, X.; He, B.C.; Wang, Y.; Chen, L.; Zuo, G.W.; Liu, B.; Bi, Y.; Huang, J.; Zhu, G.H.; et al. Establishment and characterization of a new highly metastatic human osteosarcoma cell line. *Clin. Exp. Metastasis* **2009**, *26*, 599–610. [[CrossRef](#)]
44. Chen, X.; Luther, G.; Zhang, W.; Nan, G.; Wagner, E.R.; Liao, Z.; Wu, N.; Zhang, H.; Wang, N.; Wen, S.; et al. The E-F hand calcium-binding protein S100A4 regulates the proliferation, survival and differentiation potential of human osteosarcoma cells. *Cell. Physiol. Biochem.* **2013**, *32*, 1083–1096. [[CrossRef](#)]
45. Gorska-Ponikowska, M.; Perricone, U.; Kuban-Jankowska, A.; Lo Bosco, G.; Barone, G. 2-methoxyestradiol impacts on amino acids-mediated metabolic reprogramming in osteosarcoma cells by its interaction with NMDA receptor. *J. Cell. Physiol.* **2017**, *232*, 3030–3049. [[CrossRef](#)] [[PubMed](#)]
46. Possel, H.; Noack, H.; Augustin, W.; Keilhoff, G.; Wolf, G. 2,7-Dihydrodichlorofluorescein diacetate as a fluorescent marker for peroxynitrite formation. *FEBS Lett.* **1997**, *416*, 175–178. [[CrossRef](#)]
47. Sosa, V.; Moliné, T.; Somoza, R.; Paciucci, R.; Kondoh, H.; Leonart, M.E. Oxidative stress and cancer: An overview. *Ageing Res. Rev.* **2013**, *12*, 376–390. [[CrossRef](#)]
48. Kamm, A.; Przychodzen, P.; Kuban-Jankowska, A.; Jacewicz, D.; Dabrowska, A.M.; Nussberger, S.; Wozniak, M.; Gorska-Ponikowska, M. Nitric oxide and its derivatives in the cancer battlefield. *Nitric Oxide* **2019**, *93*, 102–114. [[CrossRef](#)]
49. Bagatell, R.; Beliakoff, J.; David, C.L.; Marron, M.T.; Whitesell, L. Hsp90 inhibitors deplete key anti-apoptotic proteins in pediatric solid tumor cells and demonstrate synergistic anticancer activity with cisplatin. *Int. J. Cancer* **2005**, *113*, 179–188. [[CrossRef](#)]
50. Nagata, Y.; Anan, T.; Yoshida, T.; Mizukami, T.; Taya, Y.; Fujiwara, T.; Kato, H.; Saya, H.; Nakao, M. The stabilization mechanism of mutant-type p53 by impaired ubiquitination: The loss of wild-type p53 function and the Hsp90 association. *Oncogene* **1999**, *18*, 6037–6049. [[CrossRef](#)]
51. Bagatell, R.; Gore, L.; Egorin, M.J.; Ho, R.; Heller, G.; Boucher, N.; Zuhowski, E.G.; Whitlock, J.A.; Hunger, S.P.; Narendran, A.; et al. Phase I pharmacokinetic and pharmacodynamics study of 17-N-allylamino-17-demethoxygeldanamycin in pediatric patients with recurrent or refractory solid tumors: A pediatric oncology experimental therapeutics investigators consortium study. *Clin. Cancer Res.* **2007**, *13*, 1783–1788. [[CrossRef](#)] [[PubMed](#)]
52. Yuan, Z.; Liu, B.; Yuan, L.; Zhang, Y.; Dong, X.; Lu, J. Evidence of nuclear localization of neuronal nitric oxide synthase in cultured astrocytes of rats. *Life Sci.* **2004**, *74*, 3199–3209. [[CrossRef](#)] [[PubMed](#)]

53. Villanueva, C.; Giulivi, C. Subcellular and cellular locations of nitric oxide synthase isoforms as determinants of health and disease. *Free Radic. Biol. Med.* **2010**, *49*, 307–316. [[CrossRef](#)]
54. Aquilano, K.; Baldelli, S.; Ciriolo, M.R. Nuclear recruitment of neuronal nitric-oxide synthase by α -syn-trophin is crucial for the induction of mitochondrial biogenesis. *J. Biol. Chem.* **2014**, *289*, 365–378. [[CrossRef](#)]
55. Zhang, D.; Wang, H.; Liu, H.; Tao, T.; Wang, N.; Shen, A. nNOS Translocates into the nucleus and interacts with Sox2 to protect neurons against early excitotoxicity via promotion of Shh transcription. *Mol. Neurobiol.* **2016**, *53*, 6444–6458. [[CrossRef](#)]
56. Joly, G.A.; Ayres, M.; Kilbourn, R.G. Potent inhibition of inducible nitric oxide synthase by geldanamycin, a tyrosine kinase inhibitor, in endothelial, smooth muscle cells, and in rat aorta. *FEBS Lett.* **1997**, *403*, 40–44. [[CrossRef](#)]
57. Makondo, K.; Kamikawa, A.; Ahmed, M.; Terao, A.; Saito, M.; Kimura, K. Geldanamycin enhances hepatocyte growth factor stimulation of eNOS phosphorylation in endothelial cells. *Eur. J. Pharmacol.* **2008**, *582*, 110–115. [[CrossRef](#)]
58. Billecke, S.S.; Draganov, D.I.; Morishima, Y.; Murphy, P.J.; Dunbar, A.Y.; Pratt, W.B.; Osawa, Y. The role of Hsp90 in heme-dependent activation of apo-neuronal nitric-oxide synthase. *J. Biol. Chem.* **2004**, *279*, 30252–30258. [[CrossRef](#)] [[PubMed](#)]
59. Billecke, S.S.; Bender, A.T.; Kanelakis, K.C.; Murphy, P.J.; Lowe, E.R.; Kamada, Y.; Pratt, W.B.; Osawa, Y. Hsp90 is required for heme binding and activation of apo-neuronal nitric-oxide synthase: Geldanamycin-mediated oxidant generation is unrelated to any action of Hsp90. *J. Biol. Chem.* **2002**, *277*, 20504–20509. [[CrossRef](#)] [[PubMed](#)]
60. Song, Y.; Cardounel, A.J.; Zweier, J.L.; Xia, Y. Inhibition of superoxide generation from neuronal nitric oxide synthase by heat shock protein 90: Implications in NOS regulation. *Biochemistry* **2002**, *41*, 10616–10622. [[CrossRef](#)]
61. Pratt, W.B.; Morishima, Y.; Osawa, Y. The Hsp90 chaperone machinery regulates signaling by modulating ligand binding clefts. *J. Biol. Chem.* **2008**, *283*, 22885–22889. [[CrossRef](#)]
62. Song, Y.; Zweier, J.L.; Xia, Y. Determination of the enhancing action of HSP90 of neuronal nitric oxide synthase by EPR spectroscopy. *Am. J. Physiol. Cell Physiol.* **2001**, *281*, C1819–C1824. [[CrossRef](#)] [[PubMed](#)]
63. Song, Y.; Zweier, J.L.; Xia, Y. Heat-shock protein 90 augments neuronal nitric oxide synthase activity by enhancing Ca^{2+} /calmodulin binding. *Biochem. J.* **2001**, *355*, 357–360. [[CrossRef](#)] [[PubMed](#)]
64. Chang, Y.S.; Lo, C.W.; Sun, F.C.; Chang, M.D.; Lai, Y.K. Differential expression of Hsp90 isoforms in geldanamycin-treated 9L cells. *Biochem. Biophys. Res. Commun.* **2006**, *344*, 37–44. [[CrossRef](#)] [[PubMed](#)]
65. Chao, C.C.; Sun, F.C.; Wang, C.H.; Lo, C.W.; Chang, Y.S.; Chang, K.C.; Chang, M.D.; Lai, Y.K. Concerted actions of multiple transcription elements confer differential transactivation of HSP90 isoforms in geldanamycin-treated 9L rat gliosarcoma cells. *J. Cell. Biochem.* **2008**, *104*, 1286–1296. [[CrossRef](#)]
66. Calamia, V.; De Andrés, M.C.; Oreiro, N.; Ruiz-Romero, C.; Blanco, F.J. Hsp90 β inhibition modulates nitric oxide production and nitric oxide-induced apoptosis in human chondrocytes. *BMC Musculoskelet. Disord.* **2011**, *12*, 237. [[CrossRef](#)]
67. Kim, S.H.; Lee, S.U.; Kim, M.H.; Kim, B.T.; Min, Y.K. Mitogenic estrogen metabolites alter the expression of 17 β -estradiol-regulated proteins including heat shock proteins in human MCF-7 breast cancer cells. *Mol. Cells* **2005**, *20*, 378–384.
68. Solier, S.; Kohn, K.W.; Scroggins, B.; Xu, W.; Trepel, J.; Neckers, L.; Pommier, Y. Heat shock protein 90 α (HSP90 α), a substrate and chaperone of DNA-PK necessary for the apoptotic response. *Proc. Natl. Acad. Sci. USA* **2012**, *109*, 12866–12872. [[CrossRef](#)]
69. Longshaw, V.M.; Chapple, J.P.; Balda, M.S.; Cheetham, M.E.; Blatch, G.L. Nuclear translocation of the Hsp70/Hsp90 organizing protein mSTI1 is regulated by cell cycle kinases. *J. Cell Sci.* **2004**, *117*, 701–710. [[CrossRef](#)]
70. Passinen, S.; Valkila, J.; Manninen, T.; Syväälä, H.; Ylikomi, T. The C-terminal half of Hsp90 is responsible for its cytoplasmic localization. *Eur. J. Biochem.* **2001**, *268*, 5337–5342. [[CrossRef](#)]
71. Kim, H.R.; Kang, H.S.; Kim, H.D. Geldanamycin induces heat shock protein expression through activation of HSF1 in K562 erythroleukemic cells. *IUBMB Life* **1999**, *48*, 429–433. [[CrossRef](#)] [[PubMed](#)]
72. Karkoulis, P.K.; Stravopodis, D.J.; Konstantakou, E.G.; Voutsinas, G.E. Targeted inhibition of heat shock protein 90 disrupts multiple oncogenic signaling pathways, thus inducing cell cycle arrest and programmed cell death in human urinary bladder cancer cell lines. *Cancer Cell Int.* **2013**, *13*, 11. [[CrossRef](#)] [[PubMed](#)]

73. Kumar, S.; Stokes, J., 3rd; Singh, U.P.; Scissum Gunn, K.; Acharya, A.; Manne, U.; Mishra, M. Targeting Hsp70: A possible therapy for cancer. *Cancer Lett.* **2016**, *374*, 156–166. [[CrossRef](#)] [[PubMed](#)]
74. Myung, J.K.; Afjehi-Sadat, L.; Felizardo-Cabatic, M.; Slavic, I.; Lubec, G. Expressional patterns of chaperones in ten human tumor cell lines. *Proteome Sci.* **2004**, *2*, 8. [[CrossRef](#)]
75. Ji, F.; Lv, R.; Zhao, T. A correlation analysis between tumor imaging changes and p-AKT and HSP70 expression in tumor cells after osteosarcoma chemotherapy. *Oncol. Lett.* **2017**, *14*, 6749–6753. [[CrossRef](#)]
76. Asling, J.; Morrison, J.; Mutsaers, A.J. Targeting HSP70 and GRP78 in canine osteosarcoma cells in combination with doxorubicin chemotherapy. *Cell Stress Chaperones* **2016**, *21*, 1065–1076. [[CrossRef](#)]
77. Yun, C.H.; Yoon, S.Y.; Nguyen, T.T.; Cho, H.Y.; Kim, T.H.; Kim, S.T.; Kim, B.C.; Hong, Y.S.; Kim, S.J.; Lee, H.J. Geldanamycin inhibits TGF-beta signaling through induction of Hsp70. *Arch. Biochem. Biophys.* **2010**, *495*, 8–13. [[CrossRef](#)]
78. Powers, M.V.; Workman, P. Inhibitors of the heat shock response: Biology and pharmacology. *FEBS Lett.* **2007**, *581*, 3758–3769. [[CrossRef](#)]
79. Powers, M.V.; Workman, P. Targeting of multiple signalling pathways by heat shock protein 90 molecular chaperone inhibitors. *Endocr. Relat. Cancer* **2006**, *13*, 125–135. [[CrossRef](#)]
80. Kampinga, H.H.; Hageman, J.; Vos, M.J.; Kubota, H.; Tanguay, R.M.; Bruford, E.A.; Cheetham, M.E.; Chen, B.; Hightower, L.E. Guidelines for the nomenclature of the human heat shock proteins. *Cell Stress Chaperones* **2009**, *14*, 105–111. [[CrossRef](#)]
81. Marino Gammazza, A.; Campanella, C.; Barone, R.; Caruso Bavisotto, C.; Gorska, M.; Wozniak, M.; Carini, F.; Cappello, F.; D'Anneo, A.; Lauricella, M.; et al. Doxorubicin anti-tumor mechanisms include Hsp60 post-translational modifications leading to the Hsp60/p53 complex dissociation and instauration of replicative senescence. *Cancer Lett.* **2017**, *385*, 75–86. [[CrossRef](#)] [[PubMed](#)]



© 2020 by the authors. Licensee MDPI, Basel, Switzerland. This article is an open access article distributed under the terms and conditions of the Creative Commons Attribution (CC BY) license (<http://creativecommons.org/licenses/by/4.0/>).